Soft Matter

ARTICLE TYPE

Cite this: DOI: 00.0000/xxxxxxxxxx

Turing patterns on polymerized membranes: supplementary material (2)

Fumitake Kato,[a] Hiroshi Koibuchi,[a*] Elie Bretin,[b] Camille Carvalho,[b] Roland Denis,[b] Simon Masnou,[b] Madoka Nakayama,[c] Sohei Tasaki,[d] and Tetsuya Uchimoto[e,f]

Received Date
Accepted Date

DOI: 00.0000/xxxxxxxxxx

In this supplementary material, a detailed exposition of the numerical data on entropy and surface tension is presented. Additionally, the mean value of the coefficient of the Gaussian bond potential is presented.

1 Maximum entropy state and related phenomenons

The maximum entropy state obtained at $\lambda=\lambda_c$ is an equilibrium state with the distribution probability $\exp(-H(\lambda=\lambda_c))$ for any R_{xy} relatively close to $R_{xy}=1$. It is anticipated that this state will also manifest as an equilibrium state in real membranes. In contrast, a simulated state at $\lambda\neq\lambda_c$ is not the equilibrium state at $\lambda=\lambda_c$ because the distribution probability $\exp(-H(\lambda\neq\lambda_c))$ is different from $\exp(-H(\lambda=\lambda_c))$. It can thus be concluded that the simulated state at $\lambda\neq\lambda_c$ is considered to be a non-equilibrium state in real membranes.

If a membrane for $R_{xy}=1$ is immediately stretched to $R_{xy}=0.8$, for instance, then the internal polymer structure will gradually change to the equilibrium structure at $\lambda=\lambda_c(=0.6)$. The relaxation process in the stretched membrane is time-dependent, and therefore, cannot be simulated by the standard MC simulations. Nevertheless, the stretched membrane configuration can be captured within the canonical MC by fixing the initial λ to $\lambda<0.6$.

It is important to note that the ability to describe non-equilibrium states within the canonical modelling framework is a consequence of the incorporation of a novel IDOF, designated as $\vec{\tau}$, for the polymer structure. In the extended model, time-dependent phenomena such as relaxation can be described in terms of an equilibrium configuration by controlling $\vec{\tau}$. Moreover, the new IDOF enables an accurate representation of energy localisation resulting from the membrane stretching. The energy localisation is linked to time-dependent phenomena in Hamilton's

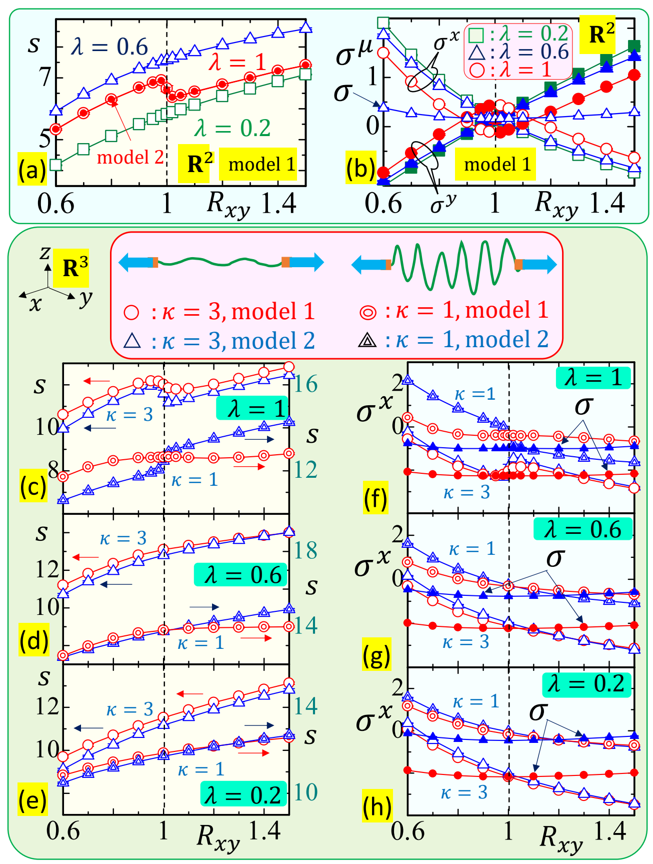

Fig. 1 (a) Entropy $s(=\delta S/\delta A_p)$ vs. R_{xy} and (b) surface tension $\sigma^\mu,(\mu=x,y)$ vs. R_{xy} of model 1 in $\mathbf{R}^2$ at $\lambda=1$ (◯), $\lambda=0.6$ (△) and $\lambda=0.2$ (□). The isotropic σ (△) for $\lambda=0.6$ is also plotted. The solid symbol (●) in (a) represents the results of model 2 at $\lambda=1$. (c)–(h) s and σ^x of models 1 and 2 in $\mathbf{R}^3$ for $\kappa=1$ and $\kappa=3$. Increasing s, plotted in (c) represents rubber elasticity. The isotropic σ is also plotted in (f),(g) and (h).

particle dynamics, as evidenced in the case that the potential energy is dependent on the space variable. Accordingly, an extended model incorporating a new IDOF is indirectly capable of repre-

[a] National Institute of Technology (KOSEN), Ibaraki College, Hitachinaka, Japan, E-mail: koi-hiro@sendai-nct.ac.jp
[b] Institut Camille Jordan (ICJ), CNRS, INSA, Universite Claude Bernard Lyon 1, Villeurbanne, France, E-mail: masnou@math.univ-lyon1.fr
[c] Tokyo Medical and Dental University, Japan
[d] Department of Mathematics, Hokkaido University, Sapporo, Japan, E-mail: tasaki@math.sci.hokudai.ac.jp
[e] Institute of Fluid Science (IFS), Tohoku University, Sendai, Japan
[f] ELyTMaX, CNRS-Universite de Lyon-Tohoku University, Sendai, Japan.

senting time-dependent phenomena, which are non-equilibrium configurations in statistical mechanical viewpoint. The source of this intriguing phenomenon can be attributed to the effective and accurate incorporation of external force-induced interaction anisotropy into the intensive components of energies, namely, $\Gamma_{ij}^{G,b}(\tau)$ and $D_{ij}^{\mu,\nu}(\tau)$ in Eqs. (5) and (6) in the main text.

Now, we plot s and the surface tension $\sigma^{\mu}, (\mu = x, y)$ vs. R_{xy}, obtained by fixing λ to $\lambda = 1$, $\lambda = 0.6$ and $\lambda = 0.2$, in Figs. 1(a)–(h), where σ^y is plotted only for models in $\mathbf{R}^2$. We observe in Fig. 1(a) that s decrease with decreasing R_{xy}. This implies that the entropy s decreases when the surface extends along the x direction. If we move to the positive direction along the R_{xy} axis in the region of $R_{xy} > 1$, we observe that s increases. This does not mean the rubber elasticity[1] because the surface is compressed along the x direction in this case.

As can be seen from Figs. 1(b), it is clear that $\sigma^x(R_{xy} < 1) > \sigma^x(R_{xy} = 1)$, which is consistent with the expectation that the surface tension increases with stretching. We find from Fig. 1(b) that σ^x exhibits a gradual increase when R_{xy} decreases from $R_{xy} = 1$ for all λ; $\lambda = 0.2$ (□), $\lambda = 0.6$ (△) and $\lambda = 1$ (○). In the region of $R_{xy} > 1$, the surface shape is oblong along the y direction, where σ^y increases. These responses of σ^x and σ^y to the stretching are physically reasonable.

Results of the models in $\mathbf{R}^3$ are plotted in Figs. 1(c)–(h), where $\lambda = 1$, $\lambda = 0.6$ and $\lambda = 0.2$. The behaviours of s and σ^x are nearly analogous to those observed in the models in $\mathbf{R}^2$. The entropy is observed to decrease under the stretching.

The isotropic σ (△) for $\lambda = 0.6$ is also plotted in Fig. 1 (b). In the case of models in $\mathbf{R}^2$, $\sigma = 0$ is satisfied when $(1/N)\sum_{ij}\Gamma_{ij}^G \ell_{ij}^2 \to 1$ from Eq. (9) in the main text under $N_{\rm fix} = 0$. This condition $\sigma = 0$ is approximately satisfied when the lattice spacing is given by $a = 0.525$, which can be varied depending on the frame area $A_p(\propto a^2)$ in the case of surfaces with a fixed boundary frame. For the models in $\mathbf{R}^3$, the condition for $\sigma = 0$ is given by $(1/N)\sum_{ij}\Gamma_{ij}^G \ell_{ij}^2 \to 3/2$ from Eq. (66) in Appendix E of the main text. However, we assume the same value of $a = 0.525$ in the simulations for the models in $\mathbf{R}^3$ independent of κ. For this reason, σ as well as σ^x is negative at $R_{xy} \to 1$ for $\kappa = 3$ in contrast to the case of the models in $\mathbf{R}^2$. Nevertheless, σ is close to σ^x at $R_{xy} \to 1$ as confirmed from Figs. 1(f)–(h).

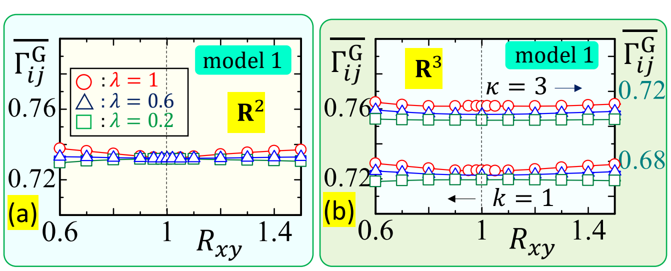

Fig. 2 $\overline{\Gamma_{ij}^G}$ vs. R_{xy} of model 1 in (a) $\mathbf{R}^2$ and (b) $\mathbf{R}^3$ for $\kappa = 3$ and $\kappa = 1$. The parameter λ is fixed to $\lambda = 1$ (○), $\lambda = 0.6$ (△) and $\lambda = 0.2$ (□).

The mean value of $\overline{\Gamma_{ij}^G} = \frac{1}{N_B}\sum_{ij}\Gamma_{ij}^G$ is plotted in Figs. 2(a),(b) for model 1 in $\mathbf{R}^2$ and $\mathbf{R}^3$, respectively. Three different values of λ are assumed for both cases of $\mathbf{R}^2$ and $\mathbf{R}^3$ as in Fig. 1. We find that $\overline{\Gamma_{ij}^G}$ is almost independent of the lattice deformation by R_{xy} in the cases of $\lambda = 0.6$ (△) and $\lambda = 0.2$ (□). In the case of $\lambda = 1$ (○), $\overline{\Gamma_{ij}^G}$ is slightly influenced by R_{xy} in the region far from $R_{xy} = 1$. It is also noteworthy that the mean values of the coefficients such as Γ_{ij}^b for the models in $\mathbf{R}^3$ and $D_{ij}^{\mu,\nu}$ are almost independent of R_{xy}.

Acknowledgements

This work is supported in part by Collaborative Research Project J24Ly01 of the Institute of Fluid Science (IFS), Tohoku University. Numerical simulations were performed on the supercomputer system AFI-NITY under the project CL01JUN24 of the Advanced Fluid Information Research Center, Institute of Fluid Science, Tohoku University.

Notes and references

1 P. J. Flory, *Molecular Theory of Rubber Elasticity*, Polymer Journal, Vol. 17, No. 1, pp 1-12 (1985), https://www.nature.com/articles/pj19851.pdf.